

Progressive Target-Styled Feature Augmentation for Unsupervised Domain Adaptation on Point Clouds

Zicheng Wang¹ Zhen Zhao² Yiming Wu¹ Luping Zhou^{2*} Dong Xu^{1*}

¹University of Hong Kong

²University of Sydney

xiaoyao3302@outlook.com {zhen.zhao, luping.zhou}@sydney.edu.au

yimingwu@hku.hk dongxu@cs.hku.hk

Abstract

Unsupervised domain adaptation is a critical challenge in the field of point cloud analysis, as models trained on one set of data often struggle to perform well in new scenarios due to domain shifts. Previous works tackle the problem by using adversarial training or self-supervised learning for feature extractor adaptation, but ensuring that features extracted from the target domain can be distinguished by the source-supervised classifier remains challenging. In this work, we propose a novel approach called progressive target-styled feature augmentation (PTSFA). Unlike previous works that focus on feature extractor adaptation, our PTSFA approach focuses on classifier adaptation. It aims to empower the classifier to recognize target-styled source features and progressively adapt to the target domain. To enhance the reliability of predictions within the PTSFA framework and encourage discriminative feature extraction, we further introduce a new intermediate domain approaching (IDA) strategy. We validate our method on the benchmark datasets, where our method achieves new state-of-the-art performance. Our code is available at <https://github.com/xiaoyao3302/PTSFA>.

1. Introduction

Deep learning on point clouds has revolutionized various real-world applications, including autonomous driving and robotics [9, 11, 25, 28, 29, 37]. However, a significant challenge arises from the domain shift, where a model trained on one set of data fails to perform well in a new scenario due to differences in scanning devices or geometry variations. To address this issue, numerous unsupervised domain adaptation methods (UDA) have been developed for point clouds. Most of these methods focus on learning a feature extractor that can extract semantically meaningful features from both domains, which can then be clas-

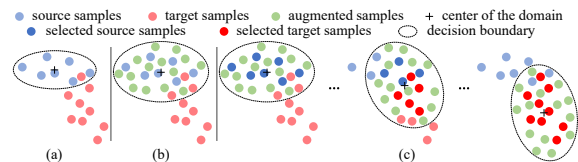


Figure 1. Illustration of our proposed progressive target-styled feature augmentation (PTSFA) approach using samples from the same category in different domains. (a) A vanilla model trained solely with source data cannot recognize certain target samples. (b) A model trained with augmented source samples will improve the generalization of the model. (c) Considering the uniqueness of each sample, we select part of the source and target samples, *i.e.*, the dark-colored ones, to progressively generate new intermediate domains toward the target domain. We construct feature augmentations towards the new intermediate domain and the model trained with augmented source samples will gradually approach the target domain.

sified by a source-supervised classifier. These methods can be broadly categorized into adversarial training-based methods [21, 32] and self-supervised learning-based methods [1, 3, 10, 16, 27, 41]. However, adversarial training encounters stability issues and lacks a guarantee of semantically meaningful feature extraction [27]. On the other hand, self-supervised tasks can primarily facilitate the learning of low-level geometry features, which may be inadequate for high-level recognition tasks, and there is no theoretical proof ensuring that the extracted features from target samples using self-supervised tasks can be distinguished by the source-supervised classifier [22, 23, 26].

In this work, different from the conventional focus on *feature extractor adaptation*, we propose a novel approach to address point cloud domain adaptation through *classifier adaptation*. Our approach involves constructing target-styled feature augmentations on the extracted source features and encouraging the classifier to recognize these target-styled source features. Although the previous work ISDA [35] has explored a similar feature augmentation strategy in the 2D domain, it cannot handle large domain gaps as it relies heavily on the estimation of the training

*Corresponding authors.

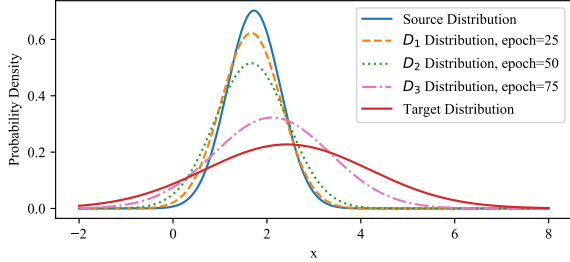


Figure 2. Visualization of the changing process of the distributions of the source, the target, and different intermediate domains. We use samples from the same category under the adaptation scenario ModelNet-10 \rightarrow ScanNet-10 as an example. D_k indicates the constructed intermediate domain during the k -th stage.

set distribution to construct augmented features [15]. Another representative 2D UDA method TSA [15] tackles the problem by constructing semantically meaningful feature augmentations towards the estimated distribution of the target domain, based on the calculation of the mean and variance of *all* target samples according to the prediction results. However, in the context of point cloud adaptation, the distances between various target samples and the source domain exhibit significant disparities [6]. These disparities result in considerable variations in prediction accuracy in the target domain, leading to *unreliable estimation of the target distribution*, which adversely affects the overall adaptation performance. In addition, some hard samples that lie far away from the source domain may also be ambiguous for the classification boundaries. As a result, it is not feasible to treat each target sample equally in the distribution estimation process.

To overcome the challenges, in this work, considering the uniqueness of each sample, we introduce a new *sample-wise* classifier adaptation approach on point clouds called progressive target-styled feature augmentation (PTSFA). Our approach involves creating a series of intermediate domains between the source domain and the target domain, and we encourage the model to progressively approach the intermediate domains to avoid direct adaptation across a significant domain gap [13]. During the process, we select samples based on their prediction scores, and we progressively decrease the selected source samples and increase the selected target samples. Then we generate intermediate domains gradually moving towards the target domain based on the selected samples, *i.e.*, the dark-colored circles in Fig. 1 (c). By progressively performing the feature augmentations on the source features towards the new intermediate domain, we encourage the model to progressively recognize the augmented source features, which enables it to approach the target domain effectively. Fig. 2 clearly demonstrates that the distribution of the newly constructed intermediate domains can progressively approach the target distribution.

In addition, considering that the prediction accuracy of

the target samples will greatly influence the estimation of the distribution [17], based on our progressively estimated intermediate domains, we further introduce a new intermediate domain approaching (IDA) strategy for *feature extractor adaptation*. We encourage features extracted from the source samples and the target samples to approach the mean of the distribution of the intermediate domain. Our IDA strategy can be combined with our PTSFA approach to encourage the model to generate more discriminative features and prevent the model from generating outlier features that might degrade the prediction accuracy, which will eventually boost the adaptation performance.

In contrast to the previous methods that rely on adversarial training or self-supervised learning for feature extractor adaptation, our classifier adaptation method is motivated by feature augmentation, which is further enhanced by our introduced feature extractor adaptation strategy. We conducted extensive experiments on several benchmark datasets to demonstrate the effectiveness of our approach. In summary, our contributions are threefold:

- We tackle unsupervised domain adaptation on point clouds from a new perspective of classifier adaptation by using target-styled feature augmentations, where we propose a progressive target-styled feature augmentation (PTSFA) approach to enable progressive adaptation of the model from the source domain to the target domain.
- We further introduce an intermediate domain approaching (IDA) strategy for feature extractor adaptation, which boosts the adaptation performance of our PTSFA approach.
- Our method achieves state-of-the-art (SOTA) performance on 3D UDA benchmark datasets, surpassing the existing methods by a significant margin.

2. Related Work

2.1. Deep Learning on Point Clouds

Inspired by PointNet [19] which directly extracts features from the unordered point sets using a set of multi-layer perceptions (MLPs), extensive deep models have been proposed [20, 34, 40], which aim at using MLPs to extract local features from the point sets hierarchically and then gather the local features to obtain the global features for point cloud recognition. While these methods have achieved remarkable performance in different scenarios, a learned model using a certain set of training data can hardly perform well in a new scenario.

2.2. Unsupervised Domain Adaptation on Point Clouds

Various methods have been proposed to tackle the unsupervised domain adaptation (UDA) problem on point clouds and most of these methods can be categorized into two

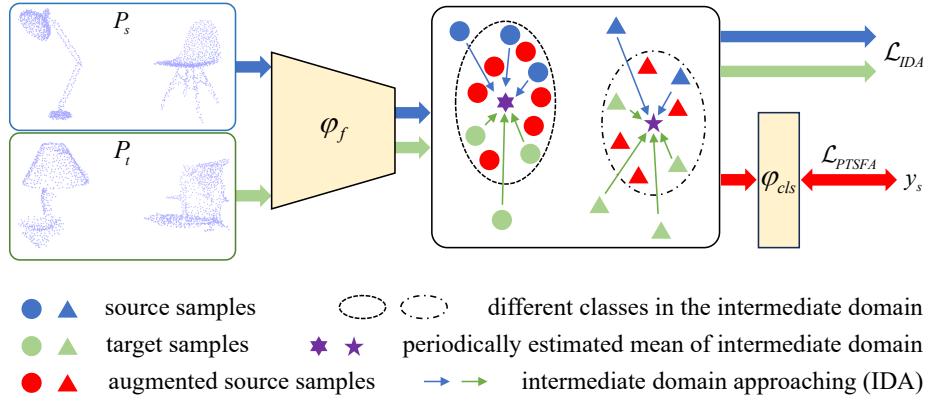


Figure 3. An overview of our proposed method for unsupervised domain adaptation on point clouds. We progressively generate intermediate domains that gradually resemble the target domain. Taking one intermediate domain as an example, we first propose a progressive target-styled feature augmentation (PTSFA) approach to construct semantically meaningful feature augmentations on the source features extracted by φ_f towards the intermediate domain, which is then fed into the classifier φ_{cls} to generate source predictions. The source predictions are supervised by the ground-truth labels y_s . Directly optimizing the corresponding \mathcal{L}_{PTSFA} enables the classifier to be adapted toward the intermediate domain. We further propose an intermediate domain approaching (IDA) strategy to encourage the features extracted from the source samples and the target samples to approach the estimated mean of the intermediate domain using \mathcal{L}_{IDA} . Our IDA strategy enables the feature extractor to be adapted towards the intermediate domain, which improves the intermediate domain estimation accuracy and further boosts the adaptation performance of our PTSFA.

main categories, *i.e.*, the adversarial-training (AT)-based methods [21, 32] and self-supervised learning (SSL)-based methods [1, 3, 10, 16, 27, 41]. The AT-based methods aim at learning a feature extractor to extract domain-invariant features from both source samples and target samples that cannot be distinguished by a domain discriminator. However, adversarial learning is not stable, and the semantic meaning of the features extracted can hardly be guaranteed, which leads to an unsatisfactory adaptation performance [27]. The SSL-based methods aim at designing self-supervised tasks to enable the feature extractor to extract semantically meaningful features from the target samples, which are then delivered to the classifier supervised by the source labels for classification. However, self-supervised learning tasks can only help the model to learn low-level geometry features that are not suitable for high-level recognition tasks like recognition [22, 23, 26]. Moreover, there is no theoretical proof that the features extracted from the target sample are suitable for classification by a source-supervised classifier.

2.3. Target-Styled Feature Augmentation

Augmentation is a widely used technique that can efficiently increase the generalization of the model [24]. Compared with previous data augmentation methods that are complex and have limited generalization ability [14], ISDA [35] is a representative 2D work that proposed to construct semantically meaningful feature augmentations with different directions to expand the decision region of the classifier so as to improve the generalization of the model. However, ISDA cannot handle large domain gaps as it can only construct feature augmentations based on the estimation of the distribution of the given training data [15].

TSA [15] is another representative 2D work that tackles the problem by using the estimated distribution of the target domain as the direction of the feature augmentations to construct target-styled feature augmentations and then perform classifier adaptation. However, TSA directly takes all of the target data for distribution estimation, while in the 3D domain, the distance between different samples and the source domain varies significantly. Directly estimating the target distribution with all of the target predictions will inevitably lead to estimation bias, which will adversely affect the overall adaptation performance.

3. Method

In this section, we present our proposed method in detail. First, we introduce the problem formulation of this work in Sec. 3.1. Then, we elaborate our newly proposed progressive target-styled feature augmentation (PTSFA) approach, which consists of a progressive target-approaching in Sec. 3.2, and a target-styled feature augmentation in Sec. 3.3. We further present our intermediate domain approaching (IDA) strategy in Sec. 3.4. Finally, the overall training loss is given in Sec. 3.5 and the pipeline of our method is illustrated in Fig. 3.

3.1. Problem Formulation

Following previous works [1, 10, 21, 27], we tackle unsupervised domain adaptation on point clouds from the perspective of classification. Specifically, we are given a set of source data $\mathbb{S} = \{\mathcal{P}_n^s, y_n^s\}_{n=1}^{N_s}$, indicating N_s point clouds \mathcal{P}_n^s in total with their corresponding category labels y_n^s . Each point cloud sample $\mathcal{P}_n^s \in \mathbb{R}^{m \times 3}$ consists

of m unordered points with their corresponding 3D coordinates. Similarly, we are given another set of target data $\mathbb{T} = \{\mathcal{P}_n^t, y_n^t\}_{n=1}^{N_t}$, while the target labels y_n^t are only available during the inference stage. All of the samples from the source and the target domain share the same label space $\mathcal{Y} = \{1, 2, \dots, C\}$. We aim at learning a model $\varphi = \varphi_f \circ \varphi_{cls}$ that can perform well on the target domain, where φ_f indicates the feature extractor and φ_{cls} indicates the classifier.

As mentioned in [2, 15, 31, 33], deep features learned by a model are usually linearized, thus it is feasible to construct augmentations in the feature space towards a certain direction to transfer the semantics of the features. Facing the UDA problem, as the distributions of the source data and the target data are different, we aim to construct feature augmentations on source samples toward the target domain. The classifier would be adapted toward the target domain by performing supervision on the target-styled source features.

Given the source data \mathcal{P}_n^s , it is easy to extract the corresponding features \mathbf{f}_n^s from each sample by $\mathbf{f}_n^s = \varphi_f(\mathcal{P}_n^s)$. Similarly, we can extract target features $\mathbf{f}_n^t = \varphi_f(\mathcal{P}_n^t)$ from the target data \mathcal{P}_n^t . In this work, we construct two *feature pools* $\mathbb{F}_s = \{\mathbf{f}_n^s\}_{n=1}^{N_s}$ to store \mathbf{f}_n^s and $\mathbb{F}_t = \{\mathbf{f}_n^t\}_{n=1}^{N_t}$ to store \mathbf{f}_n^t . Given an extracted feature \mathbf{f}_n and a classifier φ_{cls} , we can obtain the corresponding prediction $\xi_n = \varphi_{cls}(\mathbf{f}_n)$. Therefore, we can construct two *confidence score pools* $\mathbb{Z}_s = \{\zeta_n^s\}_{n=1}^{N_s}$ and $\mathbb{Z}_t = \{\zeta_n^t\}_{n=1}^{N_t}$, where $\zeta_n = \max_c \xi_n$, c indicates the index of the category. Finally, we construct two *label pools* $\mathbb{H}_s = \{\eta_n^s\}_{n=1}^{N_s}$ and $\mathbb{H}_t = \{\eta_n^t\}_{n=1}^{N_t}$, where $\eta_n^s = y_n^s$ as we have ground-truth labels available for each source sample, and $\eta_n^t = \arg \max_c \xi_n^t$, indicating the corresponding pseudo-label of each target sample. According to the corresponding η_n , we can divide the pools into category-wise feature pools as \mathbb{F}_s^c and \mathbb{F}_t^c , and confidence score pools as \mathbb{Z}_s^c and \mathbb{Z}_t^c . It is easy to estimate the mean and the covariance of the source and target distributions, *i.e.*, μ_s^c and Σ_s^c , μ_t^c and Σ_t^c , according to the source labels or the target pseudo-labels.

3.2. Progressive Target-Approaching

Recall that we aim to construct feature augmentations on the source samples toward the target domain to perform classifier adaptation. The first issue to determine is the *direction of the feature augmentations*. Different from the previous works like TSA [15] that directly estimate the augmentation direction by $\Delta\mu_c = \mu_t^c - \mu_s^c$, we argue that directly adapting the model across a significant domain gap may hamper the adaptation performance, as the estimation of the target distribution would be swayed by the incorrect target predictions, especially during the initial training stages. Moreover, the distances between various target samples and the source domain exhibit significant disparities, some hard

samples that lie far away from the source domain may be ambiguous for the classification boundaries. To address the concerns, we propose a new progressive target-approaching strategy to divide the whole training process into several stages with each stage consisting of τ training epochs. Considering that the total training epoch is T , the whole training process can be divided into $\lceil T/\tau \rceil$ stages, where $\lceil \cdot \rceil$ is a round-up operation. We construct one new intermediate domain D_k between the source and the target domain for each stage. With the intermediate domains progressively approaching the target domain, the model is encouraged to approach the intermediate domains from the source domain toward the target domain. During each stage, we aim to select samples that are closest to the mean of the current intermediate domain. This operation ensures the domain gap between two consecutive intermediate domains is small, preserving the prediction accuracy of the target samples. Consequently, this approach enhances the estimation of the new intermediate domain estimation and contributes significantly to the overall adaptation performance. Intuitively, the distance between a sample and the mean of the intermediate domain can be reflected by the prediction score ζ_n , and a higher ζ_n usually indicates that the sample may probably lie within the decision region of the classifier, with a short distance to mean of the intermediate domain. Consequently, we only select the samples with the highest ζ_n from both domains to construct the new intermediate domain.

Moreover, considering the inherent long-tailed distribution of the dataset, we propose a new ratio-based category-wise sample selection strategy to select a fixed ratio of samples from each category, aiming to pick σ^s samples from each category of the source domain and σ^t samples from each category of the target domain. Here σ^s and σ^t represent the proportion of the number of samples we wish to select from each category. To implement this, we sort \mathbb{Z}_s^c and \mathbb{Z}_t^c and keep the former σ^s source samples and the former σ^t source samples from each category. In addition, as our objective is to create target-styled feature augmentation, we advocate for the progressive convergence of the intermediate domain towards the target domain. To achieve this, we progressively decrease the number of the selected source samples and increase the number of the selected target samples, *i.e.*, $\sigma_{k+1}^s = \sigma_k^s - \Delta\sigma^s$ and $\sigma_{k+1}^t = \sigma_k^t + \Delta\sigma^t$, where k indicates the k -th intermediate domain construction stage and $\Delta\sigma$ indicates the proportional change during each stage. This approach results in a gradual shift by considering fewer source samples and more target samples to construct the intermediate domain, ensuring a progressive approach toward the target domain. It is easy to estimate the mean and covariance of the newly constructed intermediate domain as μ_k^c and Σ_k^c . During each training stage, the augmentation direction is estimated by $\Delta\mu_k^c = \mu_k^c - \mu_s^c$.

3.3. Target-Styled Feature Augmentation

After determining the direction of the feature augmentation, the next issue to determine is the *formulation of the feature augmentation*. Given an estimated distribution of the intermediate domain $N(\boldsymbol{\mu}_k^c, \boldsymbol{\Sigma}_k^c)$, it can be represented by $N(\boldsymbol{\mu}_s^c + \Delta\boldsymbol{\mu}_k^c, \boldsymbol{\Sigma}_k^c)$, where $\Delta\boldsymbol{\mu}_k^c = \boldsymbol{\mu}_k^c - \boldsymbol{\mu}_s^c$. Recall that the mean of a distribution stands for its semantics and the covariance of a distribution stands for its semantic variations. As we aim at constructing target-styled source features, we can generate M augmentations sampled from a distribution $N(\Delta\boldsymbol{\mu}_k^c, \boldsymbol{\Sigma}_k^c)$ on a certain source feature \mathbf{f}_n^s . That is, augmented source features $\tilde{\mathbf{f}}_{n,m}^s, m = 1 \cdots M$ conform to a distribution of $N(\mathbf{f}_n^s + \Delta\boldsymbol{\mu}_k^c, \boldsymbol{\Sigma}_k^c)$, which share the same semantics and variations as the constructed intermediate domain. Following [35] and [15], we also use a parameter λ to control the strength of the augmentation, *i.e.*, $\lambda\boldsymbol{\Sigma}_k^c$, to enable the semantic variants to approach the target distribution progressively, where $\lambda = (t/T) \times \lambda_0$, t and T indicate the current training epoch and the total training epoch, respectively. Considering that a linear classifier φ_{cls} is defined by a weight matrix $\mathbf{W} = [\mathbf{w}_1, \mathbf{w}_2, \cdots, \mathbf{w}_C]^T$ and a bias vector $\mathbf{b} = [b_1, b_2, \cdots, b_C]^T$, we can perform supervision on the augmented source features by minimizing \mathcal{L}_M as:

$$\mathcal{L}_M = \frac{1}{N_s} \sum_{n=1}^{N_s} \frac{1}{M} \sum_{m=1}^M -\log \left(\frac{e^{\mathbf{w}_{y_n^s}^\top \tilde{\mathbf{f}}_{n,m}^s + b_{y_n^s}}}{\sum_{c=1}^C e^{\mathbf{w}_c^\top \tilde{\mathbf{f}}_{n,m}^s + b_c}} \right). \quad (1)$$

Directly constructing M augmentations and optimizing \mathcal{L}_M is difficult to implement. However, if we construct infinite augmentations $\tilde{\mathbf{f}}_{n,m}^s$, it is easy to obtain an upper bound of \mathcal{L}_M as \mathcal{L}_{PTSFA} , which can be written as:

$$\lim_{M \rightarrow \infty} \mathcal{L}_M \leq \mathcal{L}_{PTSFA} = \frac{1}{N_s} \sum_{n=1}^{N_s} -\log \left(\frac{\vartheta_{n,s,t}^{y_n^s}}{\sum_{c=1}^C \vartheta_{n,s,t}^c} \right), \quad (2)$$

where \mathcal{L}_{PTSFA} is a standard cross-entropy (CE) loss with

$$\begin{aligned} \vartheta_{n,s,t}^c &= \mathbf{w}_c^\top \mathbf{f}_n^s + \left(\mathbf{w}_c^\top - \mathbf{w}_{y_n^s}^\top \right) \Delta\boldsymbol{\mu}_k^c \\ &+ \frac{\lambda}{2} \left(\mathbf{w}_c^\top - \mathbf{w}_{y_n^s}^\top \right) \boldsymbol{\Sigma}_k^c \left(\mathbf{w}_c^s - \mathbf{w}_{y_n^s}^s \right). \end{aligned} \quad (3)$$

Note that $\mathbf{w}_c^\top \mathbf{f}_n^s$ indicates the c -th prediction score of ξ_n^s . It is efficient to perform classifier adaptation by directly optimizing \mathcal{L}_{PTSFA} . A detailed proof is provided in the supplements.

It should be noted that different from TSA [15], we divide the training process into several stages, and update the pools \mathbb{F} , \mathbb{H} and \mathbb{Z} as well as $\boldsymbol{\mu}_s^c$ and $\boldsymbol{\Sigma}_s^c$, $\boldsymbol{\mu}_t^c$ and $\boldsymbol{\Sigma}_t^c$ at the beginning of each stage, while each training stage consists of τ epochs. In this way, we can ensure a fixed augmentation direction during each stage, which keeps the training stable.

3.4. Intermediate Domain Approaching

Our PTSFA performs classifier adaptation, a key issue of which is the estimation of the augmentation direction that relies heavily on the accuracy of the target predictions. Therefore, we further propose a new intermediate domain approaching (IDA) strategy for feature extractor adaptation, which can be combined with our PTSFA for a better adaptation performance. In particular, we aim at enabling the source features and the target features to approach the mean of the intermediate domain. Specifically, given the extracted source features \mathbf{f}_n^s , the extracted target features \mathbf{f}_n^t , and the estimated mean of the intermediate domain $\boldsymbol{\mu}_k^c$, we encourage \mathbf{f}_n^s and \mathbf{f}_n^t to approach the $\boldsymbol{\mu}_k^c$ of the corresponding category while staying far from the $\boldsymbol{\mu}_k^c$ of other categories. To achieve this, we formulate our IDA loss as:

$$\mathcal{L}_{IDA}^s = \frac{1}{N_s} \sum_{n=1}^{N_s} -\log \left(\frac{\exp \left(\cos \left(\mathbf{f}_n^s, \boldsymbol{\mu}_k^c \right) / \kappa \right)}{\sum_{c=1}^C \exp \left(\cos \left(\mathbf{f}_n^s, \boldsymbol{\mu}_k^c \right) / \kappa \right)} \right), \quad (4)$$

and

$$\mathcal{L}_{IDA}^t = \frac{1}{N_t} \sum_{n=1}^{N_t} -\log \left(\frac{\exp \left(\cos \left(\mathbf{f}_n^t, \boldsymbol{\mu}_k^c \right) / \kappa \right)}{\sum_{c=1}^C \exp \left(\cos \left(\mathbf{f}_n^t, \boldsymbol{\mu}_k^c \right) / \kappa \right)} \right), \quad (5)$$

where κ is the temperature value [7, 39]. Optimizing \mathcal{L}_{IDA}^s and \mathcal{L}_{IDA}^t will on one hand promote feature extractor adaptation, preventing the encoder from generating outlier features, and on the other hand encourage the encode to extract more discriminative features. This enhances the adaptation performance of our PTSFA method.

3.5. Overall Objective

To sum up, our newly proposed method consists of a classifier adaptation method PTSFA and a feature extractor adaptation method IDA, and the total loss can be written as:

$$\mathcal{L} = \alpha \mathcal{L}_{PTSFA} + \beta \mathcal{L}_{IDA}^s + \gamma \mathcal{L}_{IDA}^t, \quad (6)$$

where α , β and γ are the trade-off parameters. A detailed introduction to our training process is provided in the supplements.

4. Experiments

4.1. Datasets

We adopt the widely used 3D unsupervised domain adaptation (UDA) benchmark datasets **PointDA-10 dataset** [21] and **GraspNetPC-10 dataset** [27] to validate the effectiveness of our method. More details about the datasets are provided in the supplements.

Methods	AD	FA	SSL	PS	M → S	M → S*	S → M	S → S*	S* → M	S* → S	Avg.
Oracle					93.9	78.4	96.2	78.4	96.2	93.9	89.5
w/o DA					83.3	43.8	75.5	42.5	63.8	64.2	62.2
DANN [12]	✓				74.8	42.1	57.5	50.9	43.7	71.6	56.8
PointDAN [21]	✓				83.9	44.8	63.3	45.7	43.6	56.4	56.3
ISDA [33]		✓			84.3	52.9	82.4	50.1	67.3	70.0	67.8
TSA [15]		✓			85.1	50.3	86.9	46.4	76.9	74.7	70.0
RS [26]			✓		79.9	46.7	75.2	51.4	71.8	71.2	66.0
DefRec+PCM [1]			✓		81.7	51.8	78.6	54.5	73.7	71.1	68.6
GAST [41]			✓		83.9	56.7	76.4	55.0	73.4	72.2	69.5
ImplicitPCDA [27]			✓		<u>85.8</u>	55.3	77.2	55.4	73.8	72.4	70.0
DAPS [36]			✓		84.6	59.2	77.1	56.0	73.1	76.2	70.8
Ours		✓			86.6	58.5	87.9	59.7	85.1	80.9	76.5
GAST [41]			✓	✓	84.8	59.8	80.8	56.7	81.1	74.9	73.0
MLSP [16]			✓	✓	83.7	55.4	77.1	55.6	78.2	76.1	71.0
ImplicitPCDA [27]			✓	✓	86.2	58.6	81.4	56.9	81.5	74.4	73.2
GLRV [10]			✓	✓	85.4	60.4	78.8	57.7	77.8	76.2	72.7
MLSP [16]			✓	✓	86.2	59.1	<u>83.5</u>	57.6	81.2	76.4	74.0
FD [3]			✓	✓	83.9	<u>61.1</u>	80.3	58.9	85.5	80.9	75.1
DAPS [36]			✓	✓	86.9	59.7	78.7	55.5	82.0	80.5	73.9
DAS* [36]			✓	✓	87.2	60.5	82.4	58.1	84.8	<u>82.3</u>	<u>75.9</u>
Ours		✓		✓	88.0	61.7	89.3	60.2	89.0	84.4	78.8

Table 1. Comparison of classification accuracies (in %) with the state-of-the-art 3D UDA methods on the PointDA-10 dataset. The best performance is highlighted in bold and the previous best result is underlined. The abbreviations *AD*, *FA*, *SSL*, and *PS* correspond to adversarial domain alignment, feature augmentation, self-supervised learning, and pseudo-labeling, respectively. The symbol * denotes utilization of a more sophisticated pseudo-labeling method that requires more parameters during the fine-tuning stage.

4.2. Implementation Details

We follow the previous works [1, 27, 41] and adopt DGCNN [34] as our backbone. We set the number of labeled data and unlabeled data as 8 within each mini-batch. The training epoch T is set as 100 and the training epoch of each intermediate domain construction stage τ is set as 5, indicating the training process can be divided into 20 stages. The temperature parameter κ is set as 2.0. λ_0 that controls the semantic variants is set as 0.25, which is adopted from TSA [15]. The trade-off parameters α , β , and γ are all set as 1.0 by default, respectively. More detailed experiment settings are provided in the supplements.

4.3. Experimental Results

We compare our method with recent state-of-the-art (SOTA) UDA methods, including adversarial domain alignment-based methods (AD) like DANN [12] and PointDAN [21], feature augmentation-based methods (FA) like ISDA [33] and TSA [15], and self-supervised learning-based methods (SSL) like RS [26], DefRec+PCM [1], GAST [41], ImplicitPCDA [27], GLRV [10], MLSP [16], FD [3] and DAS [36]. As some methods adopt a pseudo-labeling method (PS) for the model fine-tuning, we report their performance both with and without using PS fine-tuning, corresponding to the lower and upper portions of Tab. 1 and Tab. 2, respectively. It is noteworthy that as DAS employed a more sophisticated PS method, which requires more parameters during training or inference, we also report its performance with the traditional PS method,

denoted as DAPS. In addition, we compare with the supervised learning method directly training the model with only labeled source data for reference (denoted as “w/o DA”), as well as the Oracle method that trains the model by using labeled target data (denoted as “Oracle”).

The results on the PointDA-10 dataset are reported in Tab. 1. As can be seen, our method surpasses the current SOTA methods by a large margin under all six adaptation scenarios. The average recognition accuracy of our method outperforms the current SOTA method DAS by a notable margin of 2.9%, while DAS employs a more sophisticated PS method to fine-tune the performance. Our advantage over DAS can be further enlarged to 4.9% or 5.7% when comparing ours with DAS using the traditional PS (*i.e.*, DAPS) or without PS. Moreover, our method demonstrates notable superiority over the two feature augmentation-based methods ISDA [33] and TSA [15], with improvements of 8.7% over ISDA and 6.5% over TSA. This verifies the effectiveness of our progressive target-styled feature augmentation strategy.

The results on the GraspNetPC-10 dataset are reported in Tab. 2. Consistently, our method surpasses the w/o DA method by over 30% and also outperforms the current SOTA method DAS, despite that DAS requires more parameters for a more complicated PS fine-tuning. Our method without PS fine-tuning wins the second-best performer DAPS by a large margin of 6.9%. Moreover, compared with the two feature augmentation-based methods ISDA and TSA, our method demonstrated overwhelming advantages with almost or more than 15% improvements.

Methods	AD	FA	SSL	PS	Syn. \rightarrow Kin.	Syn. \rightarrow RS.	Kin. \rightarrow RS.	RS. \rightarrow Kin.	Avg.
Oracle					97.2	95.6	95.6	97.2	96.4
w/o DA					61.3	54.4	53.4	68.5	59.4
DANN [12]	✓				78.6	70.3	46.1	67.9	65.7
PointDAN [21]	✓				77.0	72.5	65.9	82.3	74.4
ISDA [33]			✓		79.5	65.0	65.3	80.8	72.7
TSA [15]			✓		77.8	60.0	57.7	85.2	70.2
RS [26]				✓	67.3	58.6	55.7	69.6	62.8
DefRec+PCM [1]				✓	80.7	70.5	65.1	77.7	73.5
GAST [41]				✓	69.8	61.3	58.7	70.6	65.1
ImplicitPCDA [27]				✓	81.2	73.1	66.4	82.6	75.8
DAPS [36]				✓	91.6	74.2	71.9	85.0	80.7
Ours		✓			94.2	83.5	75.9	96.8	87.6
GAST [41]			✓	✓	81.3	72.3	61.3	80.1	73.8
ImplicitPCDA [27]			✓	✓	94.6	80.5	76.8	85.9	84.4
DAPS [36]			✓	✓	97.0	79.6	79.1	95.7	87.8
DAS* [36]			✓	✓	97.2	84.4	79.9	97.0	89.6
Ours		✓		✓	97.5	84.9	80.1	97.9	90.1

Table 2. Comparison of classification accuracies (in %) with the state-of-the-art 3D UDA methods on the GraspNetPC-10 dataset. The best performance is highlighted in bold and the previous best result is underlined. The abbreviations *AD*, *FA*, *SSL*, and *PS* correspond to adversarial domain alignment, feature augmentation, self-supervised learning, and pseudo-labeling, respectively. The symbol * denotes utilization of a more sophisticated pseudo-labeling method that requires more parameters during the fine-tuning stage.

TSFA	IDA	PTA	M \rightarrow S	M \rightarrow S*	S \rightarrow M	S \rightarrow S*	S* \rightarrow M	S* \rightarrow S	Avg.
			83.3	43.8	75.5	42.5	63.8	64.2	62.2
✓			86.8	57.4	85.5	56.0	80.8	79.3	74.3
	✓		85.3	52.2	80.7	55.8	68.5	72.6	69.2
✓	✓		84.2	54.3	81.3	55.0	65.5	71.3	68.6
✓		✓	87.5	58.2	88.4	58.3	82.1	79.4	75.7
	✓	✓	86.6	55.7	84.7	55.7	81.9	79.1	74.0
✓	✓	✓	86.6	58.5	87.9	59.7	85.1	80.9	76.5

Table 3. Ablation study on the effectiveness of different components in our method, including the basic target-styled feature augmentation (TSFA), our progressive target-approaching (PTA) strategy, and our intermediate domain approaching (IDA) strategy. Experiments are conducted on the PointDA-10 dataset.

Note that our FA-based method surpasses the current AD-based methods and SSL-based methods by a large margin, indicating the great potential of the feature augmentations in tackling UDA problems.

4.4. Ablation Study

In this section, we single out the contributions of our module designs on the PointDA-10 dataset. Note that our method includes a progressive target-styled feature augmentation (PTSFA) approach for classifier adaptation and an intermediate domain approaching (IDA) method for feature extractor adaptation, and our PTSFA further consists of a basic target-styled feature augmentation (TSFA) and a progressive target-approaching (PTA) strategy. Also note that our PTA strategy is a general training strategy that can also be combined with our IDA method. The results of the ablation study are reported in Tab. 3. It can be clearly seen from the table that the basic TSFA will improve the average accuracy of the backbone DGCNN model by 12.1%, which surpasses TSA [15] as we adopt a more stable training strategy. Applying our IDA alone will bring a performance improvement of 7.0% over the w/o DA method. However, when combining our TSFA and IDA, the performance drops

to only 68.6%. The main reason is that the domain gap between the source domain and the target domain is huge and the above-mentioned two methods both rely heavily on the estimation of the target domain. Directly adapting the model across such a large domain gap will inevitably lead to incorrect distribution estimation, harming the adaptation performance of the model.

It can also be inferred from the table that both the combination of our TSFA with our PTA strategy and the combination of our IDA with our PTA strategy can bring performance improvements of 1.4% and 4.8%, respectively. More importantly, combining the three components TSFA, IDA and PTA will bring further improvements of 0.8% and 2.5%, respectively, from TSFA+PTA and IDA+PTA. The main reason is that we decompose the huge domain gap into a set of small domain gaps by introducing a set of intermediate domains, ensuring an accurate intermediate domain estimation. These results clearly verify the importance and effectiveness of our PTA strategy. Moreover, it can be seen from the table that only deploying our TSFA and PTA, *i.e.*, our PTSFA method, can also outperform the current SOTA method DAPS by a large margin of 4.9%.

We further delve into the intricate design of our PTA

decreasing source	increasing target	M \rightarrow S	M \rightarrow S*	S \rightarrow M	S \rightarrow S*	S* \rightarrow M	S* \rightarrow S	Avg.
		86.8	57.4	85.5	56.0	80.8	79.3	74.3
	✓	87.5	58.4	85.9	56.9	79.3	77.3	74.7
✓		87.1	56.3	89.1	58.1	82.1	79.8	75.4
✓	✓	87.5	58.2	88.4	58.3	82.1	79.4	75.7

Table 4. Ablation study on the effectiveness of different strategies related to our progressive target-approaching (PTA) strategy, including progressively decreasing the selected source samples (decreasing source) and progressively increasing the selected target samples (increasing target). Experiments are conducted on the PointDA-10 dataset. Note that the IDA module is not included.

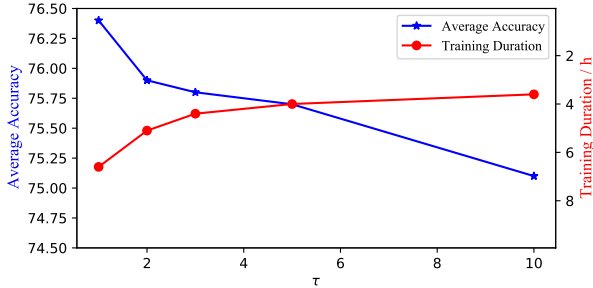


Figure 4. Ablation study on the sensitivity of our method to the training epoch at each intermediate domain construction stage, *i.e.*, τ . Experiments are conducted on the PointDA-10 dataset. We report the average recognition accuracy on the target domain and the average training duration.

strategy. As a reminder, our approach involves a continual reduction in the number of selected source samples and a simultaneous increase in the number of selected target samples throughout the training process. We thereby scrutinize the effectiveness of each strategy, as reported in Tab. 4. As seen, when decreasing the number of the selected source samples while keeping all of the target samples for intermediate domain construction, the model would gradually approach the target domain. In particular, our “decreasing source” strategy exhibits great performance under Real-to-Sim scenarios like $S^* \rightarrow M$ and $S^* \rightarrow S$. The main reason could be that the samples from the source domain contain noise, which can potentially introduce disruptive information and undermine the model’s recognition capabilities. Progressively reducing these samples will help prevent the model from being misled by the noise. Moreover, when increasing the number of the selected target samples while keeping all source samples for intermediate domain construction, the adaptation performance on the Sim-to-Real scenarios like $M \rightarrow S^*$ and $S \rightarrow S^*$ will be improved. The main reason could be that our “increasing target” strategy would expand the decision region of the classifier, thus improving the recognition performance of the model on the target domain. The results clearly verified the effectiveness of our PTA strategy.

In addition, we analyze the sensitivity of our method to the number of epochs (τ) that the intermediate domain construction stage lasts, as depicted in Fig. 4. From the figure, it is evident that a more frequent intermediate domain construction stage results in improved adaptation per-

κ	0.05	0.1	0.5	1.0	2.0	3.0	5.0	10.0
Avg.	73.4	73.2	74.2	75.1	76.5	76.0	76.0	76.0

Table 5. Ablation study on the sensitivity of our method to the temperature parameter, *i.e.*, κ . Experiments are conducted on the PointDA-10 dataset and we only report the average recognition accuracy on the target domain (Avg.).

formance, as it allows for a more precise estimation of augmentation direction. However, the high update frequency comes with increased training costs, as it requires an additional inference stage at the beginning of each intermediate domain construction phase to estimate the augmentation direction. The figure clearly illustrates that constructing a new intermediate domain per epoch would more than double the training time compared to constructing one intermediate domain every 10 epochs, while the performance improvement is limited. Taking into account both training costs and performance, we decided to perform the intermediate construction stage every 5 epochs.

Finally, we analyze the sensitivity of our method to the temperature κ , as reported in Tab. 5. It can be clearly seen from the table that our method is robust to such a parameter. When $\kappa = 2.0$, our model achieves the best overall recognition performance of 76.5% on the target domain.

Limitation: Neglecting the great adaptation performance of our method, our method requires an extra inference stage at the beginning of each intermediate domain construction stage, and we also require extra space to store the pools \mathbb{F} , \mathbb{H} and \mathbb{Z} during the training stage, which will introduce more training costs. Nevertheless, our method requires no extra costs during the inference stage.

5. Conclusion

In this work, we have presented a new progressive target-styled feature augmentation method to tackle unsupervised domain adaptation on point clouds from a new perspective of classifier adaptation. We further come up with an intermediate domain approaching strategy for feature extractor adaptation, which can be combined with our classifier adaptation method to achieve better adaptation performance. Extensive experiments on the benchmark datasets have validated the effectiveness of our newly proposed approaches, where our method outperforms the current state-of-the-art methods by a large margin.

References

- [1] Idan Achituve, Haggai Maron, and Gal Chechik. Self-supervised learning for domain adaptation on point clouds. In *Proceedings of the IEEE/CVF Winter Conference on Applications of Computer Vision*, pages 123–133, 2021. [1](#), [3](#), [6](#), [7](#), [12](#)
- [2] Yoshua Bengio, Grégoire Mesnil, Yann Dauphin, and Salah Rifai. Better mixing via deep representations. In *International conference on machine learning*, pages 552–560. PMLR, 2013. [4](#)
- [3] Adriano Cardace, Riccardo Spezialetti, Pierluigi Zama Ramirez, Samuele Salti, and Luigi Di Stefano. Self-distillation for unsupervised 3d domain adaptation. In *Proceedings of the IEEE/CVF Winter Conference on Applications of Computer Vision*, pages 4166–4177, 2023. [1](#), [3](#), [6](#)
- [4] David Chandler. Introduction to modern statistical. *Mechanics. Oxford University Press, Oxford, UK*, 5:449, 1987. [11](#)
- [5] Angel X Chang, Thomas Funkhouser, Leonidas Guibas, Pat Hanrahan, Qixing Huang, Zimo Li, Silvio Savarese, Manolis Savva, Shuran Song, Hao Su, et al. Shapenet: An information-rich 3d model repository. *arXiv preprint arXiv:1512.03012*, 2015. [11](#)
- [6] Chaoqi Chen, Weiping Xie, Wenbing Huang, Yu Rong, Xinghao Ding, Yue Huang, Tingyang Xu, and Junzhou Huang. Progressive feature alignment for unsupervised domain adaptation. In *Proceedings of the IEEE/CVF conference on computer vision and pattern recognition*, pages 627–636, 2019. [2](#)
- [7] Ting Chen, Simon Kornblith, Mohammad Norouzi, and Geoffrey Hinton. A simple framework for contrastive learning of visual representations. In *International conference on machine learning*, pages 1597–1607. PMLR, 2020. [5](#)
- [8] Angela Dai, Angel X Chang, Manolis Savva, Maciej Halber, Thomas Funkhouser, and Matthias Nießner. Scannet: Richly-annotated 3d reconstructions of indoor scenes. In *Proceedings of the IEEE conference on computer vision and pattern recognition*, pages 5828–5839, 2017. [11](#)
- [9] Abhishek Das, Samyak Datta, Georgia Gkioxari, Stefan Lee, Devi Parikh, and Dhruv Batra. Embodied question answering. In *Proceedings of the IEEE conference on computer vision and pattern recognition*, pages 1–10, 2018. [1](#)
- [10] Hehe Fan, Xiaojun Chang, Wanyue Zhang, Yi Cheng, Ying Sun, and Mohan Kankanhalli. Self-supervised global-local structure modeling for point cloud domain adaptation with reliable voted pseudo labels. In *Proceedings of the IEEE/CVF Conference on Computer Vision and Pattern Recognition*, pages 6377–6386, 2022. [1](#), [3](#), [6](#)
- [11] Hao-Shu Fang, Chenxi Wang, Minghao Gou, and Cewu Lu. Graspnet-1billion: A large-scale benchmark for general object grasping. In *Proceedings of the IEEE/CVF conference on computer vision and pattern recognition*, pages 11444–11453, 2020. [1](#), [11](#)
- [12] Yaroslav Ganin, Evgeniya Ustinova, Hana Ajakan, Pascal Germain, Hugo Larochelle, François Laviolette, Mario Marchand, and Victor Lempitsky. Domain-adversarial training of neural networks. *The journal of machine learning research*, 17(1):2096–2030, 2016. [6](#), [7](#)
- [13] Han-Kai Hsu, Chun-Han Yao, Yi-Hsuan Tsai, Wei-Chih Hung, Hung-Yu Tseng, Maneesh Singh, and Ming-Hsuan Yang. Progressive domain adaptation for object detection. In *Proceedings of the IEEE/CVF winter conference on applications of computer vision*, pages 749–757, 2020. [2](#)
- [14] Pan Li, Da Li, Wei Li, Shaogang Gong, Yanwei Fu, and Timothy M Hospedales. A simple feature augmentation for domain generalization. In *Proceedings of the IEEE/CVF International Conference on Computer Vision*, pages 8886–8895, 2021. [3](#)
- [15] Shuang Li, Mixue Xie, Kaixiong Gong, Chi Harold Liu, Yulin Wang, and Wei Li. Transferable semantic augmentation for domain adaptation. In *Proceedings of the IEEE/CVF conference on computer vision and pattern recognition*, pages 11516–11525, 2021. [2](#), [3](#), [4](#), [5](#), [6](#), [7](#), [12](#)
- [16] Hanxue Liang, Hehe Fan, Zhiwen Fan, Yi Wang, Tianlong Chen, Yu Cheng, and Zhangyang Wang. Point cloud domain adaptation via masked local 3d structure prediction. In *European Conference on Computer Vision*, pages 156–172. Springer, 2022. [1](#), [3](#), [6](#), [12](#)
- [17] Omri Lifshitz and Lior Wolf. Sample selection for universal domain adaptation. In *Proceedings of the AAAI Conference on Artificial Intelligence*, pages 8592–8600, 2021. [2](#)
- [18] Haggai Maron, Meirav Galun, Noam Aigerman, Miri Trope, Nadav Dym, Ersin Yumer, Vladimir G Kim, and Yaron Lipman. Convolutional neural networks on surfaces via seamless toric covers. *ACM Trans. Graph.*, 36(4):71–1, 2017. [12](#)
- [19] Charles R Qi, Hao Su, Kaichun Mo, and Leonidas J Guibas. Pointnet: Deep learning on point sets for 3d classification and segmentation. In *Proceedings of the IEEE conference on computer vision and pattern recognition*, pages 652–660, 2017. [2](#)
- [20] Charles Ruizhongtai Qi, Li Yi, Hao Su, and Leonidas J Guibas. Pointnet++: Deep hierarchical feature learning on point sets in a metric space. *Advances in neural information processing systems*, 30, 2017. [2](#)
- [21] Can Qin, Haoxuan You, Lichen Wang, C-C Jay Kuo, and Yun Fu. Pointdan: A multi-scale 3d domain adaption network for point cloud representation. *Advances in Neural Information Processing Systems*, 32, 2019. [1](#), [3](#), [5](#), [6](#), [7](#), [11](#)
- [22] Yongming Rao, Jiwen Lu, and Jie Zhou. Global-local bidirectional reasoning for unsupervised representation learning of 3d point clouds. In *Proceedings of the IEEE/CVF Conference on Computer Vision and Pattern Recognition*, pages 5376–5385, 2020. [1](#), [3](#)
- [23] Yongming Rao, Jiwen Lu, and Jie Zhou. Pointglr: Unsupervised structural representation learning of 3d point clouds. *IEEE Transactions on Pattern Analysis and Machine Intelligence*, 2022. [1](#), [3](#)
- [24] Alexander J Ratner, Henry Ehrenberg, Zeshan Hussain, Jared Dunnmon, and Christopher Ré. Learning to compose domain-specific transformations for data augmentation. *Advances in neural information processing systems*, 30, 2017. [3](#)
- [25] Danila Rukhovich, Anna Vorontsova, and Anton Konushin. Tr3d: Towards real-time indoor 3d object detection. *arXiv preprint arXiv:2302.02858*, 2023. [1](#)

- [26] Jonathan Sauder and Bjarne Sievers. Self-supervised deep learning on point clouds by reconstructing space. *Advances in Neural Information Processing Systems*, 32, 2019. 1, 3, 6, 7, 12
- [27] Yuefan Shen, Yanchao Yang, Mi Yan, He Wang, Youyi Zheng, and Leonidas J Guibas. Domain adaptation on point clouds via geometry-aware implicits. In *Proceedings of the IEEE/CVF Conference on Computer Vision and Pattern Recognition*, pages 7223–7232, 2022. 1, 3, 5, 6, 7, 11, 12
- [28] Shaoshuai Shi, Xiaogang Wang, and Hongsheng Li. Point-rcnn: 3d object proposal generation and detection from point cloud. In *Proceedings of the IEEE/CVF conference on computer vision and pattern recognition*, pages 770–779, 2019. 1
- [29] Shaoshuai Shi, Chaoxu Guo, Li Jiang, Zhe Wang, Jianping Shi, Xiaogang Wang, and Hongsheng Li. Pv-rcnn: Point-voxel feature set abstraction for 3d object detection. In *Proceedings of the IEEE/CVF Conference on Computer Vision and Pattern Recognition*, pages 10529–10538, 2020. 1
- [30] Yi-Hsuan Tsai, Wei-Chih Hung, Samuel Schuster, Kihyuk Sohn, Ming-Hsuan Yang, and Manmohan Chandraker. Learning to adapt structured output space for semantic segmentation. In *Proceedings of the IEEE conference on computer vision and pattern recognition*, pages 7472–7481, 2018. 12
- [31] Paul Upchurch, Jacob Gardner, Geoff Pleiss, Robert Pless, Noah Snavely, Kavita Bala, and Kilian Weinberger. Deep feature interpolation for image content changes. In *Proceedings of the IEEE conference on computer vision and pattern recognition*, pages 7064–7073, 2017. 4
- [32] Feiyu Wang, Wen Li, and Dong Xu. Cross-dataset point cloud recognition using deep-shallow domain adaptation network. *IEEE Transactions on Image Processing*, 30:7364–7377, 2021. 1, 3
- [33] Yulin Wang, Xuran Pan, Shiji Song, Hong Zhang, Gao Huang, and Cheng Wu. Implicit semantic data augmentation for deep networks. In *Advances in Neural Information Processing Systems (NeurIPS)*, pages 12635–12644, 2019. 4, 6, 7
- [34] Yue Wang, Yongbin Sun, Ziwei Liu, Sanjay E Sarma, Michael M Bronstein, and Justin M Solomon. Dynamic graph cnn for learning on point clouds. *ACM Transactions on Graphics (tog)*, 38(5):1–12, 2019. 2, 6, 12
- [35] Yulin Wang, Gao Huang, Shiji Song, Xuran Pan, Yitong Xia, and Cheng Wu. Regularizing deep networks with semantic data augmentation. *IEEE Transactions on Pattern Analysis and Machine Intelligence*, 2021. 1, 3, 5
- [36] Zicheng Wang, Wen Li, and Dong Xu. Domain adaptive sampling for cross-domain point cloud recognition. *IEEE Transactions on Circuits and Systems for Video Technology*, 2023. 6, 7
- [37] Hai Wu, Chenglu Wen, Shaoshuai Shi, Xin Li, and Cheng Wang. Virtual sparse convolution for multimodal 3d object detection. In *Proceedings of the IEEE/CVF Conference on Computer Vision and Pattern Recognition*, pages 21653–21662, 2023. 1
- [38] Zhirong Wu, Shuran Song, Aditya Khosla, Fisher Yu, Linguang Zhang, Xiaoou Tang, and Jianxiong Xiao. 3d shapenets: A deep representation for volumetric shapes. In *Proceedings of the IEEE conference on computer vision and pattern recognition*, pages 1912–1920, 2015. 11
- [39] Xiangyu Yue, Zangwei Zheng, Shanghang Zhang, Yang Gao, Trevor Darrell, Kurt Keutzer, and Alberto Sangiovanni Vincentelli. Prototypical cross-domain self-supervised learning for few-shot unsupervised domain adaptation. In *Proceedings of the IEEE/CVF Conference on Computer Vision and Pattern Recognition*, pages 13834–13844, 2021. 5
- [40] Hengshuang Zhao, Li Jiang, Jiaya Jia, Philip HS Torr, and Vladlen Koltun. Point transformer. In *Proceedings of the IEEE/CVF international conference on computer vision*, pages 16259–16268, 2021. 2
- [41] Longkun Zou, Hui Tang, Ke Chen, and Kui Jia. Geometry-aware self-training for unsupervised domain adaptation on object point clouds. In *Proceedings of the IEEE/CVF International Conference on Computer Vision*, pages 6403–6412, 2021. 1, 3, 6, 7, 12

Progressive Target-Styled Feature Augmentation for Unsupervised Domain Adaptation on Point Clouds

Supplementary Material

6. More Details of Our Method

6.1. Target-Styled Feature Augmentation

In Sec. 3.3, we have introduced our target-styled feature augmentation approach. In this section, we show the detailed derivation of our \mathcal{L}_{TSPA} .

Recall that

$$\mathcal{L}_M = \frac{1}{N_s} \sum_{n=1}^{N_s} \frac{1}{M} \sum_{m=1}^M -\log \left(\frac{e^{\mathbf{w}_{y_n^s}^\top \mathbf{f}_{n,m}^s + b_{y_i^s}}}{\sum_{c=1}^C e^{\mathbf{w}_c^\top \mathbf{f}_{n,m}^s + b_c}} \right). \quad (7)$$

When $M \rightarrow \infty$, letting $\tilde{\mathbf{f}}_n^s$ denote the augmented source features, we can obtain

$$\begin{aligned} \lim_{M \rightarrow \infty} \mathcal{L}_M &= \frac{1}{N_s} \sum_{n=1}^{N_s} \mathbb{E}_{\tilde{\mathbf{f}}_n^s} \left[-\log \left(\frac{e^{\mathbf{w}_{y_n^s}^\top \tilde{\mathbf{f}}_n^s + b_{y_i^s}}}{\sum_{c=1}^C e^{\mathbf{w}_c^\top \tilde{\mathbf{f}}_n^s + b_c}} \right) \right] \\ &= \frac{1}{N_s} \sum_{n=1}^{N_s} \mathbb{E}_{\tilde{\mathbf{f}}_n^s} \left[\log \left(\sum_{c=1}^C e^{(\mathbf{w}_c^\top - \mathbf{w}_{y_n^s}^\top) \tilde{\mathbf{f}}_n^s + (b_c - b_{y_i^s})} \right) \right]. \end{aligned} \quad (8)$$

According to the Jensen's inequality [4], $\mathbb{E}[\log(X)] \leq \log(\mathbb{E}[X])$, we can re-write Eq. (8) as:

$$\begin{aligned} \lim_{M \rightarrow \infty} \mathcal{L}_M &\leq \frac{1}{N_s} \sum_{n=1}^{N_s} \log \left(\mathbb{E}_{\tilde{\mathbf{f}}_n^s} \left[\sum_{c=1}^C e^{(\mathbf{w}_c^\top - \mathbf{w}_{y_n^s}^\top) \tilde{\mathbf{f}}_n^s + (b_c - b_{y_i^s})} \right] \right) \\ &= \frac{1}{N_s} \sum_{n=1}^{N_s} \log \left(\sum_{c=1}^C \mathbb{E}_{\tilde{\mathbf{f}}_n^s} \left[e^{(\mathbf{w}_c^\top - \mathbf{w}_{y_n^s}^\top) \tilde{\mathbf{f}}_n^s + (b_c - b_{y_i^s})} \right] \right). \end{aligned} \quad (9)$$

As $\tilde{\mathbf{f}}_n^s$ denotes the augmented source features, where the initial source features \mathbf{f}_n^s obey $N(\boldsymbol{\mu}_{s^s}^{y_n^s}, \boldsymbol{\Sigma}_{s^s}^{y_n^s})$, it is easy to infer that $\tilde{\mathbf{f}}_n^s \sim N(\boldsymbol{\mu}_{s^s}^{y_n^s} + \Delta \boldsymbol{\mu}_t^{y_n^s}, \lambda \boldsymbol{\Sigma}_{y_n^s}^{y_n^s})$. The mean of $(\mathbf{w}_c^\top - \mathbf{w}_{y_n^s}^\top) \tilde{\mathbf{f}}_n^s + (b_c - b_{y_i^s})$ can be calculated as $(\mathbf{w}_c^\top - \mathbf{w}_{y_n^s}^\top) (\boldsymbol{\mu}_{s^s}^{y_n^s} + \Delta \boldsymbol{\mu}_t^{y_n^s}) + (b_c - b_{y_i^s})$, while the covariance of $(\mathbf{w}_c^\top - \mathbf{w}_{y_n^s}^\top) \tilde{\mathbf{f}}_n^s + (b_c - b_{y_i^s})$ can be calculated as $\lambda (\mathbf{w}_c^\top - \mathbf{w}_{y_n^s}^\top) \lambda \boldsymbol{\Sigma}_{y_n^s}^{y_n^s} (\mathbf{w}_c - \mathbf{w}_{y_n^s})$. Leveraging the function $\mathbb{E}[e^{aX}] = e^{a\mu + \frac{1}{2}a^2\sigma}$, $X \sim N(\mu, \sigma)$, it is easy to draw Eq. (2).

6.2. Overall Training

In Sec. 3.5, we have introduced the total loss function of our method. In this section, we give a more detailed introduc-

tion to our overall training process. During our implementation, we introduce a warm-up stage at the beginning of the training process to prevent inaccurate intermediate domain estimation. Specifically, during the warm-up stage, we perform the standard cross-entropy (CE) loss to supervise the source predictions as:

$$\mathcal{L}_{CE} = -\frac{1}{N_s} \sum_{n=1}^{N_s} \ell^{ce}(\boldsymbol{\xi}_n, y_n^s). \quad (10)$$

During the warm-up stage, we optimize \mathcal{L}_{CE} to train the model. After the warm-up stage, we follow Sec. 3 and optimize Eq. (6) to train the model.

7. More Experiments

7.1. Datasets

In Sec. 4.1, we have briefly introduced the datasets we used, in this section, we provide more details about the dataset.

PointDA-10 dataset [21] is the most widely used 3D unsupervised domain adaptation (UDA) benchmark dataset designed for point cloud classification. The PointDA-10 dataset consists of three subsets, ModelNet-10 (M), ShapeNet-10 (S) and ScanNet-10 (S*), which are sampled from three widely-used datasets, ModelNet [38], ShapeNet [5] and ScanNet [8], respectively. The three subsets share the same 10 categories and each sample consists of 1,024 points in total. In particular, ModelNet-10 consists of 4,183 training samples and 856 testing samples, where these samples are generated with CAD by uniformly sampling from synthetic 3D models. ShapeNet-10 consists of 17,387 training samples and 2,492 testing samples, where the samples are also generated with CAD, but the shape of the samples in ShapeNet-10 also exhibits variations from those in ModelNet-10. ScanNet-10 consists of 6,110 training samples and 1,769 testing samples, and all of the samples are scanned from real-world indoor scenarios with RGB-D cameras. The samples in ScanNet-10 are usually sparse with some missing parts because of noise and occlusion. When using the training set of one subset as the source domain, and the training set of another subset as the target domain, a total of six UDA scenarios, *i.e.*, $M \rightarrow S$, $M \rightarrow S^*$, $S \rightarrow M$, $S \rightarrow S^*$, $S^* \rightarrow M$ and $S^* \rightarrow S$, can be obtained.

GraspNetPC-10 dataset [27] is another 3D UDA benchmark dataset for point cloud classification, which is created from GraspNet [11] and consists of four subsets,

Methods	F → A	F → MI	F → SP	MI → A	MI → F	MI → SP	A → F	A → MI	A → SP	SP → A	SP → F	SP → MI	Avg.
Oracle	80.9	81.8	82.4	80.9	84.0	82.4	84.0	81.8	82.4	80.9	84.0	81.8	82.3
w/o DA	78.5	60.9	66.5	26.6	33.6	69.9	38.5	31.2	30.0	74.1	68.4	64.5	53.6
Adapt-SegMap [30]	70.5	60.1	65.3	49.1	<u>54.0</u>	62.8	44.2	<u>35.4</u>	35.1	70.1	67.7	63.8	56.5
RS [26]	78.7	60.7	66.9	59.6	38.4	70.4	44.0	30.4	36.6	70.7	<u>73.0</u>	65.3	57.9
DefRec+PCM [1]	79.7	<u>61.8</u>	<u>67.4</u>	67.1	40.1	<u>72.6</u>	42.5	28.9	32.2	66.4	72.2	66.2	58.1
MLSP [16]	80.9	60.0	65.5	<u>67.3</u>	40.4	70.8	<u>45.4</u>	31.1	<u>38.4</u>	<u>74.8</u>	72.5	<u>66.6</u>	<u>59.5</u>
Ours	77.5	62.2	67.9	71.5	57.8	66.8	56.5	48.6	52.0	69.8	76.3	69.9	64.7

Table 6. Comparison of segmentation accuracies (mean IoU) with the state-of-the-art 3D UDA methods on the PointSegDA dataset. The best performance is highlighted in bold and the previous best result is underlined.

i.e., two synthetic subsets and two scanned subsets. The synthetic samples in GraspNetPC-10 are re-projected from rendered synthetic scenes while the real depth scanned samples in GraspNetPC-10 are captured by two different depth cameras, *i.e.*, Kinect2 and Intel Realsense, constituting two real-world domains. The subsets also share the same 10 categories. Each sample consists of 1,024 points in total. In particular, the synthetic domain (Syn.) contains 12,000 training samples. The Kinect real-world domain (Kin.) contains 10,973 training samples and 2,560 testing samples while the Realsense real-world domain (RS) contains 10,698 training samples and 2,560 testing samples. When using one subset as the source domain, and another scanned subset as the target domain, a total of four DA scenarios, *i.e.*, Syn. → Kin., Syn. → RS., Kin. → RS. and RS. → Kin. can be obtained.

In addition, we follow previous works [1, 16] and report the results on the **PointSegDA dataset**, a 3D UDA benchmark dataset for point cloud part segmentation. PointSegDA dataset is created from [18] and consists of four subsets, *i.e.*, FAUST (F), MIT (MI), ADOBE (A), and SCAPE (SP). The subsets share the same 8 categories of human body parts. Each sample from the PointSegDA dataset consists of 2,048 points in total. When using the training set of one subset as the source domain and the training set of another subset as the target domain, a total of twelve UDA scenarios, *i.e.*, FAUST → ADOBE, FAUST → MIT, FAUST → SCAPE, MIT → ADOBE, MIT → FAUST, MIT → SCAPE, ADOBE → FAUST, ADOBE → MIT, ADOBE → SCAPE, SCAPE → ADOBE, SCAPE → FAUST, and SCAPE → MIT, can be obtained.

7.2. Implementation details

In Sec. 4.2, we have listed the main experimental settings, in this section, we provide the detailed implementation details of our method.

Following the previous works [1, 27, 41], we adopt DGCNN [34] as our backbone but simplify the last classifier to a single linear layer, following TSA [15]. In addition, we use a simple max-pooling operation to replace the combination of a max-pooling operation and an average-pooling operation to avoid the over-fitting problem. Our models are trained on a server with four NVIDIA GTX 2080Ti GPUs, except for the PointSegDA dataset, where our methods are

trained on a server with ten NVIDIA RTX 3090 GPUs. We only use one GPU per experiment. Our implementation is based on the PyTorch framework. For all experiments, we use the Adam optimizer together with an epoch-wise cosine annealing learning rate scheduler initiated with a learning rate of 0.001 and a weight decay of 0.00005. We train all of our models for 100 epochs setting the numbers of both labeled data and unlabeled data as 8 within each mini-batch. Notably, the 100 training epochs include a 10-epoch warm-up stage. Each intermediate domain construction stage consists of 5 epochs ($\tau = 5$). The initial ratio for selecting source data (σ^s) is set as 1.0, while the initial ratio for selecting target data (σ^t) is set as 0.0 and the proportional changes $\Delta\sigma^s$ and $\Delta\sigma^t$ are both set as 0.05. The temperature parameter κ is set as 2.0, and λ_0 that controls the semantic variants is set as 0.25, which is adopted from TSA [15]. The trade-off parameters α , β , and γ are all set as 1.0, respectively.

In addition, following the previous work [41], we fine-tune our learned model under a self-paced learning (SPL) paradigm where we set the initial threshold for selecting confident predictions as 0.8, and the increasing step as 0.01. The 2BDA training stage consists of 10 training circles and each circle consists of 10 epochs. Most of our experiment settings are adopted from [27, 41].

7.3. Experimental Results

In this section, we benchmark our method against recent state-of-the-art (SOTA) UDA methods on the PointSegDA dataset. In addition, we provide a comparison with the supervised learning method directly training the model with only labeled source data for reference (denoted as “w/o DA”), as well as the Oracle method that trains the model by using labeled target data (denoted as “Oracle”). The results are reported in Tab. 6. Note that all methods are implemented without using the pseudo-labeling fine-tuning method. It can be clearly seen that our method has demonstrated significant performance improvements under most transfer scenarios. For instance, under the A → F scenario, our method outperforms the current state-of-the-art (SOTA) method MLSP by 11.1%. In addition, under the A → MI scenario, our method achieves a performance gain of 13.2% compared to MLSP. On average, our method outperforms the current SOTA method by over 5% on the PointSegDA

source approaching	target approaching	M \rightarrow S	M \rightarrow S*	S \rightarrow M	S \rightarrow S*	S* \rightarrow M	S* \rightarrow S	Avg.
	✓	87.5	58.2	88.4	58.3	82.1	79.4	75.7
✓		87.1	57.1	89.6	59.6	82.9	80.9	76.1
✓	✓	86.9	56.6	89.9	58.6	83.8	81.1	76.2
	✓	86.6	58.5	87.9	59.7	85.1	80.9	76.5

Table 7. Ablation study on the effectiveness of different strategies in our new intermediate domain approaching (IDA) strategy, including approaching source samples with the new intermediate domain (source approaching) and approaching target samples with the new intermediate domain (target approaching). Experiments are conducted on the PointDA-10 dataset.

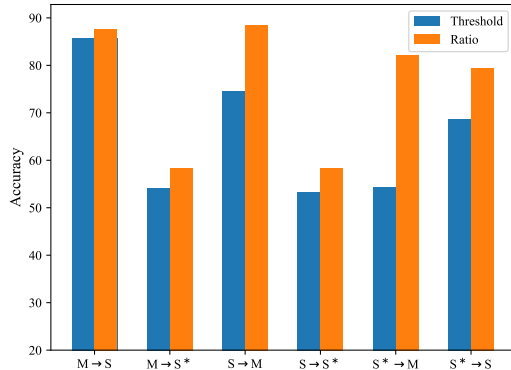


Figure 5. Ablation study on the effectiveness of our newly proposed ratio-based category-wise sample selection strategy (Ratio) and the classic threshold-based sample selection strategy (Threshold). Experiments are conducted on the PointDA-10 dataset.

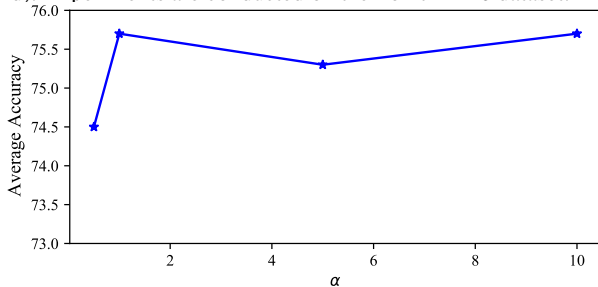


Figure 6. Ablation study on the sensitivity of our method to the trade-off parameters, *i.e.*, α , β and γ , where $\beta = 1.0$ and $\gamma = 1.0$. Experiments are conducted on the PointDA-10 dataset and we only report the average recognition accuracy on the target domain.

dataset, showcasing the tremendous potential of our approach.

7.4. Ablation Study

In this section, we carry on more ablation studies to verify the effectiveness of our approach.

We first validate the effectiveness of our newly proposed ratio-based category-wise sample selection strategy by comparing it with the conventional threshold-based sample selection strategy. The results are presented in Fig. 5. Our ratio-based category-wise sample selection strategy significantly outperforms the threshold-based approach. This notable improvement can be attributed to the limita-

Method	Accuracy (%)	Training Time (h)
w/o DA	62.2	3.0
Ours	75.7	3.8

Table 8. Ablation study on the relationship between the performance and the training costs of our approach and the “w/o DA” method. Experiments are conducted on the PointDA-10 dataset. We report the average recognition accuracy on the target domain and the average training duration.

tions of threshold-based sample selection strategies, which fail to ensure a gradual increase in the number of selected samples. Consequently, the constructed intermediate domain may diverge significantly from the source domain, resulting in a substantial domain gap. In contrast, our strategy effectively mitigates the risk of a large domain gap, ensuring accurate estimation of the intermediate domain and enhancing classifier adaptation performance. Furthermore, setting a higher threshold at the outset of the training process leads to the exclusion of a considerable number of samples, exacerbating the confirmation bias issue and adversely affecting training stability and model performance, as shown in the figure under the S* \rightarrow M and S* \rightarrow S scenarios.

Then, we scrutinize the design of our IDA strategy, and the results are reported in Tab. 7. As a reminder, we encourage both the source and the target features to approach the mean of the intermediate domain to perform feature extractor adaptation. As seen, both the source and the target approaching strategies prevent the model from generating outlier features, especially on noisy domains like S*. Moreover, as the intermediate domain gradually approaches the target domain, the source approaching strategy enables the source features extracted by the feature extractor to gradually approach the target domain, which can lead to feature extractor adaptation, bringing a better adaptation performance.

In addition, we conducted an analysis to evaluate the sensitivity of our method to the trade-off parameters α , β and γ . As β and γ control the weights of the \mathcal{L}_{IDA}^s and \mathcal{L}_{IDA}^t , respectively, we argue that these two loss functions contribute equally to the training process. Therefore, we set both β and γ to 1.0 and vary the value of α . The average accuracies over six adaptation scenarios are reported in Fig. 6. It is evident that our method exhibits robustness to the trade-off parameters. Varying the value of α within a reasonably large range does not significantly impact the adaptation per-

formance of our approach. This indicates that our method is not overly sensitive to the choice of trade-off parameters and maintains stable performance across different parameter settings.

We further investigate the relationship between the performance and the training costs of our approach and report the results in Tab. 8. It is evident that our method achieves significant improvement in adaptation performance compared to the “w/o DA” method, with only a modest increase of approximately 25% in training costs.